



Geniposide effectively safeguards HT22 cells against A β -induced damage by activating mitophagy via the PINK1/Parkin signaling pathway

Jiayi Ye^{a,1}, Jiaying Wu^{a,1}, Liang Ai^{a,1}, Min Zhu^a, Yun Li^b, Dong Yin^{b,*}, Qihui Huang^{a,*}

^a Sun Yat-sen Memorial Hospital, Sun Yat-sen University, Guangzhou 510300, PR China

^b Guangdong Provincial Key Laboratory of Malignant Tumor Epigenetics and Gene Regulation, Guangdong-Hong Kong Joint Laboratory for RNA Medicine, Research Center of Medicine, Sun Yat-Sen Memorial Hospital, Sun Yat-Sen University, Guangzhou 510120, PR China

ARTICLE INFO

Keywords:

Geniposide
Alzheimer's disease
Mitophagy
PINK1/Parkin pathway

ABSTRACT

Alzheimer's disease (AD) is a neurodegenerative disorder characterized by the significant involvement of amyloid-beta (A β) peptide in its pathogenesis. Geniposide, derived from the versatile medicinal of *Gardenia jasminoides*, is one of the active compounds studied extensively. The objective was to explore the impact of geniposide on A β ₂₅₋₃₅-induced damage in HT22 cells, specifically focusing on its modulation of PINK1/Parkin-mediated mitophagy. In our investigation, geniposide exhibited remarkable restorative effects by enhancing cell viability and preserving the mitochondrial membrane potential. Moreover, it effectively reduced and mitigated the oxidative stress and apoptosis rates induced by A β ₂₅₋₃₅. Notably, geniposide exhibited the capacity to enhance autophagic flux, upregulate LC3II and Beclin-1 expression, and downregulate the expression of p62. Furthermore, geniposide positively influenced the expression of PINK1 and Parkin proteins, with molecular docking substantiating a strong interaction between geniposide and PINK1/Parkin proteins. Intriguingly, the beneficial outcomes of geniposide on alleviating the pronounced apoptosis rates, the overproduction of reactive oxygen species, and diminished the PINK1 and Parkin expression induced by A β ₂₅₋₃₅ were compromised by the mitophagy inhibitor cyclosporine A (CsA). Collectively, these findings suggested that geniposide potentially shields HT22 cells against neurodegenerative damage triggered by A β ₂₅₋₃₅ through the activation of mitophagy. The insights contribute valuable references to the defensive consequences against neurological damage of geniposide, thereby highlighting its potential as a therapeutic intervention in AD.

1. Introduction

Alzheimer's disease (AD) is a neurodegenerative condition associated with the aging process. It is characterized by a gradual decline in cognitive function and the development of neuropsychiatric symptoms. In addition, AD is often characterized by neuronal death and morphological and biochemical changes in brain tissue, such as the formation of neurofibrillary tangles and amyloid plaques [1]. According to a nationwide study, there are more than 15.07 million individuals aged 60 and above diagnosed with dementia in China. Among them, AD patients account for 65.2 % of the total cases [2,3]. AD has become a significant public health issue globally. Despite extensive basic and clinical

research, a therapeutic strategy for the treatment of AD has not been found yet. Existing medications for AD provide limited improvement in cognitive symptoms, but they are unable to halt the progression of the disease [4]. As a result, there is an urgent need to explore effective neuroprotective drugs for the treatment of AD.

The buildup of dysfunctional mitochondria is a characteristic feature of the aging process and age-related neurodegenerative disorders, such as AD [5]. Mitochondrial dysfunction has been identified as an early manifestation in the onset of AD, and impaired clearance of damaged mitochondria may exacerbate the pathological changes in AD [6,7]. Mitophagy is a critical process through which cells selectively degrade and eliminate malfunctioning mitochondria, ensuring cellular health

Abbreviations: AD, Alzheimer's disease; A β , Amyloid-beta; CQ, chloroquine; CsA, cyclosporine A; GE, Geniposide; MMP, Mitochondrial membrane potential; ATP, Adenosine triphosphate; PI, Propidium iodide; ROS, Reactive oxygen species; PPI, Protein-protein interaction; GO, Gene ontology; PDB, Protein data bank; ANOVA, Analysis of variance; BP, Biological processes; CC, Cellular components; MF, Molecular functions; Mdivi-1, Mitochondrial division inhibitor 1.

* Corresponding authors.

E-mail addresses: yind3@mail.sysu.edu.cn (D. Yin), huangqih@mail.sysu.edu.cn (Q. Huang).

¹ These authors contribute to this work equally.

<https://doi.org/10.1016/j.bcp.2024.116296>

Received 12 January 2024; Received in revised form 12 May 2024; Accepted 15 May 2024

Available online 16 May 2024

0006-2952/© 2024 The Authors. Published by Elsevier Inc. This is an open access article under the CC BY-NC-ND license (<http://creativecommons.org/licenses/by-nc-nd/4.0/>).

and functioning optimally [8]. Currently, the PINK1/Parkin-mediated pathway stands out as the most extensively researched form of mitophagy [9]. Studies have shown that restoring mitophagy can reduce the production of A β and have a positive influence on neuronal recovery [10]. Furthermore, mitophagy enhancers such as urolithin A and actinonin have achieved good therapeutic effects in cell cultures and AD mice [10]. Some natural compounds such as kaempferol and rhapontigenin could induce neuronal mitophagy in a PINK1-dependent manner while reducing A β pathology [11]. Natural products that activate PINK1-dependent mitophagy may be acknowledged as a novel therapeutic intervention for AD.

Gardenia is a widely used medicinal plant in traditional medicine. Geniposide (GE), as one of the iridoid glycosides found in Gardenia fruit, possesses multiple pharmacological properties [12]. Numerous scientific studies have illustrated that GE exhibits antioxidant [13], anti-apoptotic [14], and neuroprotective properties [15]. Fig. 1 shows the chemical structure of GE. The current literature suggests that GE could inhibit mitochondrial oxidative stress in APP/PS1 mice [16], restore mitochondrial membrane potential (MMP) levels in A β -induced primary neurons [17], and alleviate neuronal damage. Furthermore, GE could regulate the mTOR signaling pathway to attenuate cognitive dysfunction and cerebral dysfunction in APP/PS1 mice [18], enhance autophagy levels and reduce A β_{1-40} plaque deposition in mice [19], and improve AD-specific neuropathological damage. In spite of that, it is unclear whether GE could regulate mitophagy through the PINK1/Parkin signaling pathway to exert neuroprotective effects. Therefore, we investigated the effectiveness and potential mechanisms of GE in A β -induced HT22 cells. Our results implied that GE alleviated A β -induced neurotoxicity in HT22 cells, and its beneficial implications appear to be associated with mitophagy mediated by the PINK1/Parkin signaling pathway.

2. Materials and methods

2.1. A β_{25-35} and drug preparation

The preparation method of A β_{25-35} (MCE; New Jersey, USA) was carried out according to a previously established protocol [20]. Briefly, A β_{25-35} was dissolved in ddH₂O at a concentration of 200 μ M and

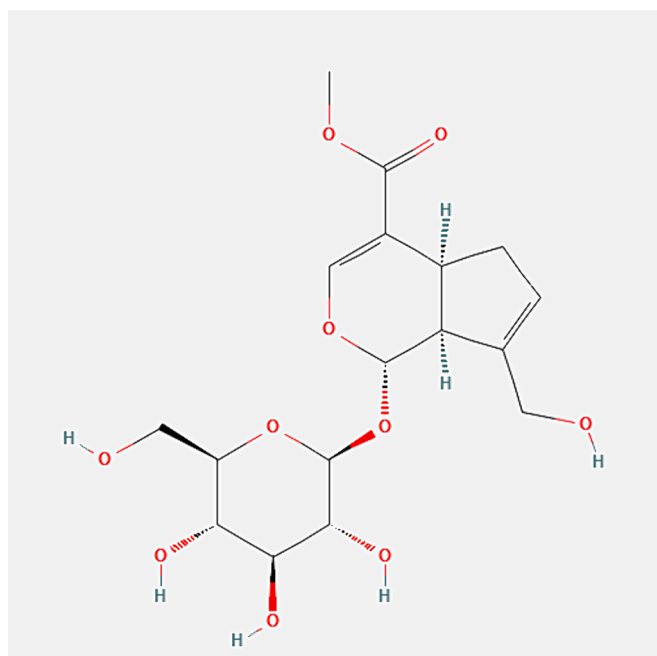


Fig. 1. Chemical structures of geniposide (GE).

allowed to incubate at 37 °C for 7 days to encourage the aggregation of peptide molecules. The resulting aggregated A β_{25-35} solution was then stored at -20 °C for later use. Prior to experimentation, the aggregated A β_{25-35} solution was diluted with a basal medium to achieve the desired concentration. On the other hand, GE (Solarbio; Beijing, China) was dissolved in DMSO and preserved at -80 °C for future utilization.

2.2. Cell culture and cell treatment

HT22 cells were kindly provided by Professor Jun Liu (Sun Yat-sen University; Guangdong, China). The HT22 cell line was cultivated in DMEM medium at a temperature of 37 °C and under 5 % CO₂ atmosphere. To investigate the potential protective impacts of GE on neurons, the cells were exposed to varying concentrations of GE for 1 h prior to experimentation. Following pre-treatment, the cells were incubated for an additional 24 h in the presence or absence of A β_{25-35} . To investigate the influence of A β on autophagic flux in HT22 cells, we employed the autophagy inhibitor chloroquine (CQ; Aladdin; Los Angeles, USA) to assess the expression of LC3 protein in A β -induced HT22 cells. Furthermore, in order to explore the impact of mitophagy pathway mediated by GE in A β -induced HT22 cells, we utilized the mitophagy inhibitors cyclosporine A (CsA; MCE) and Mitochondrial division inhibitor 1 (Mdivi-1; MCE) to evaluate their effects on the expression of mitophagy pathway-related proteins in A β -induced HT22 cells.

2.3. Cell viability assessment

Cell viability was assessed using the CCK-8 assay (APEX-BIO; Houston, USA) as per the recommended protocols from the manufacturer. In a nutshell, the cells were treated with a 10 μ L solution of CCK-8 and incubated at 37 °C for 2 h. The absorbance of the samples was then measured at 450 nm using a multifunctional microplate reader. (TECAN Spark10M; Männedorf, Switzerland).

2.4. Cell apoptosis assay and Hoechst 33,342 fluorescence staining

The detection of cell apoptosis induced by A β_{25-35} was performed following the manufacturer's recommended procedures using an annexin V-FITC/propidium iodide (PI) double staining kit (Uelandy; Shanghai, China) and flow cytometry (Beckman CytoFLEX S; California, USA). Firstly, the cells were trypsinized and then the cells were stained by dual staining and the extent of cell apoptosis was assessed by flow cytometry. Additionally, morphological changes of apoptotic cells were evaluated by staining the cells with Hoechst 33,342 (Beyotime; Shanghai, China) and observing them under the fluorescence microscope (Olympus IX71; Tokyo, Japan).

2.5. Evaluation of reactive oxygen species (ROS) concentrations

The level of ROS was measured using the DCFH-DA (Beyotime) fluorescent probe. To perform the assay, diluted DCFH-DA was added to the cells and incubated at 37 °C. The cells were then examined under the fluorescence microscope to determine the levels of ROS.

2.6. Assessment of the mitochondrial membrane potential (MMP)

To determine the MMP, we employed the MMP assay kit (4A Biotech; Beijing, China) with the fluorescent probe JC-10. HT22 cells were incubated with the JC-10 fluorescent probe based on the instructions provided by the manufacturer. Subsequently, the cells were visualized utilizing a fluorescence microscope.

2.7. Immunofluorescence

In the immunofluorescence experiment, HT22 cells were incubated with Mito-Tracker Red CMXRos (Beyotime) for 30 min. Following that,

the cells were fixed in 4 % paraformaldehyde (HUAYUN; Guangdong, China), followed by a 20-minute reaction with Triton X-100 (Beyotime). After that, the cells were incubated with an immunofluorescence blocking solution (Beyotime). Then, the cells were incubated with Parkin (1:200; Proteintech; Wuhan, China) or LC3 (1:500; Proteintech) antibody overnight. Subsequently, the cells were incubated with the fluorescent secondary antibody (1:500; Proteintech). Finally, the samples were mounted with an anti-fluorescence quenching mounting (HUAYUN) medium and observed under the Leica microscope (Mica; Wetzlar, Germany).

2.8. Protein-protein interaction (PPI) network and gene ontology (GO) enrichment analysis

The target genes of GE were extracted from the TCMSP database [21] (<https://tcmspw.com/tcmsp.php>). To identify the key genes affected by GE, we uploaded these target genes to the UniProt database [22] (<https://www.UniProt.org/>), specifically restricted to *Homo sapiens* (Human). The disease-related genes were predominantly selected from the DisGeNET [23] (<https://www.disgenet.org/>) and GeneCards databases [24] (<https://www.genecards.org/>), limited to the *Homo sapiens* species. The intersection of GE and AD genes was visualized by the Venn diagram (<https://bioinformatics.psb.ugent.be/webtools/Venn/>).

Subsequently, the genes were uploaded to the STRING database [25] (<https://string-db.org>), where we focused exclusively on *Homo sapiens*. We generated a PPI network diagram using the minimum interaction score of 0.400. To gain insights into the biological significance of these genes, we performed an enrichment analysis of relevant GO terms using the DAVID database [26] (<https://david.ncifcrf.gov/>). Finally, we visualized the results through the Bioinformatics platform (<https://www.bioinformatics.com.cn/>).

2.9. Molecular docking

To investigate the potential binding modes of GE with PINK1 and Parkin proteins, molecular docking analysis was conducted using AutoDock software. Initially, the protein data bank (PDB) file of the receptor was downloaded from the PDB database [27] (<https://www.rcsb.org/>), while the 3D structure file of the ligand was obtained from the PubChem database [28] (<https://pubchem.ncbi.nlm.nih.gov>). Subsequently, AutoDock Tools 1.5.7 was utilized to adjust the coordinates and dimensions of the Grid Box for the docking process between the receptor and ligand. Afterward, the configuration achieving the highest score was chosen for additional analysis, and the docking outcomes were visualized using PyMol 4.6.0.

2.10. Western blot

To collect total proteins from cells, lysis buffer (Beyotime) was used, and the cells were kept on ice during the process. The mixture was then centrifuged at 13,000 rpm. The mitochondrial proteins of HT22 cells were extracted with cell mitochondria isolation kit (Beyotime) according to the manufacturer's protocol. The protein concentration was determined using a BCA protein assay kit (EpiZyme; Massachusetts, USA). Subsequently, the samples were separated on SDS-PAGE and transferred onto PVDF membranes (Merck millipore; Massachusetts, USA). The membranes were subjected to an overnight at 4°C with primary antibodies against Beclin-1, caspase-3, p62 (1:1000; Abclonal; Wuhan, China), PINK1 (1:1000; Proteintech), LC3 (1:2500; Proteintech), GAPDH (1:10000; Proteintech) and Parkin. Afterward, the membranes were incubated with corresponding secondary antibodies (1:10000; Proteintech) for 1 h. Finally, the immunoreactive bands were visualized using an ECL detection reagent (Beyotime). The relative band intensities were normalized to GAPDH or COXIV as an internal reference. Densitometry analysis was performed using the Image J software.

2.11. Statistics analysis

The data are presented as mean ± SEM. Statistical significance among multiple groups was determined using either one-way analysis of variance (ANOVA) or Bonferroni multiple comparison test with GraphPad Prism 8.0.2 software. A *P*-value of less than 0.05 was considered statistically significant.

3. Results

3.1. GE enhances cell viability of $A\beta_{25-35}$ -induced HT22 cells

HT22 cells, widely used in neurobiology research, are mouse hippocampal neuronal cells. Initially, we conducted the CCK-8 assay to evaluate the neurotoxic concentration of $A\beta_{25-35}$ and determine the appropriate neuroprotective concentration of GE. Fig. 2A illustrated that $A\beta_{25-35}$ exhibited dose-dependent suppression of cell viability, with a notable reduction of approximately 50 % observed at 40 μ M. Hence, we utilized the concentration of 40 μ M $A\beta_{25-35}$ to establish an AD cell model by subjecting the cells to a 24-hour treatment. Fig. 2B demonstrated that GE concentrations below 40 μ M did not have adverse effects on cell viability. At 40 μ M concentration, GE resulted in a cell viability of 90.6 %. Consequently, we selected a concentration range of 5–40 μ M GE for subsequent experiments. Fig. 2C and 2D showed that pre-treatment with GE at 20 μ M and 40 μ M concentrations, combined with $A\beta_{25-35}$ treatment for 24 h, significantly improved cell viability and enhanced neuronal density and morphology. Therefore, we employed concentrations of 20 μ M and 40 μ M GE for subsequent experimental investigations as neuroprotective concentrations.

3.2. GE alleviates $A\beta_{25-35}$ -induced apoptosis

To further validate the neuroprotective influence of GE against $A\beta_{25-35}$ -induced neurotoxicity, we utilized flow cytometry and Hoechst 33,342 staining to scrutinize cellular apoptosis. As depicted in Fig. 3A and C, $A\beta_{25-35}$ markedly augmented the incidence of apoptosis in cells, provoking characteristic morphological alterations like chromatin condensation and nuclear shrinkage. Nevertheless, pretreatment with GE counteracted these changes by mitigating cell apoptosis and ameliorating nuclear morphology. In addition, we assessed the levels of cleaved caspase-3, as an indicator of cellular apoptosis. Post-treatment with $A\beta_{25-35}$ (40 μ M), there was a notable increase in the Cleaved caspase-3 proteins expression (Fig. 3E and F). Notably, pretreatment with GE significantly decreased the expression levels of Cleaved caspase-3 proteins. Thus, pretreatment with GE holds the potential to reverse $A\beta_{25-35}$ -induced apoptosis.

3.3. GE mitigates $A\beta_{25-35}$ -induced impairment of mitochondrial function and oxidative stress levels

To investigate the potential of GE to inhibit cell apoptosis through its antioxidant effects, we evaluated intracellular levels of ROS and MMP. As depicted in Fig. 4A and B, $A\beta_{25-35}$ treatment significantly increased ROS levels, while pretreatment with GE resulted in the restoration of ROS levels. This finding suggests that GE pretreatment can effectively reduce the elevated ROS induced by $A\beta_{25-35}$. Moreover, our qualitative and quantitative analyses (Fig. 4C and D) revealed that $A\beta_{25-35}$ caused a decrease in MMP, which was subsequently restored by GE pretreatment. Collectively, these results revealed that GE has the potential to alleviate $A\beta_{25-35}$ -induced oxidative stress by improving mitochondrial function.

3.4. GE reverses $A\beta_{25-35}$ -induced inhibition of autophagy

Inhibition of cellular autophagy can result in excessive generation of ROS and a decline in MMP. To confirm whether autophagy flux impairment occurred in $A\beta$ -induced HT22 cells, CQ (CQ, an inhibitor of

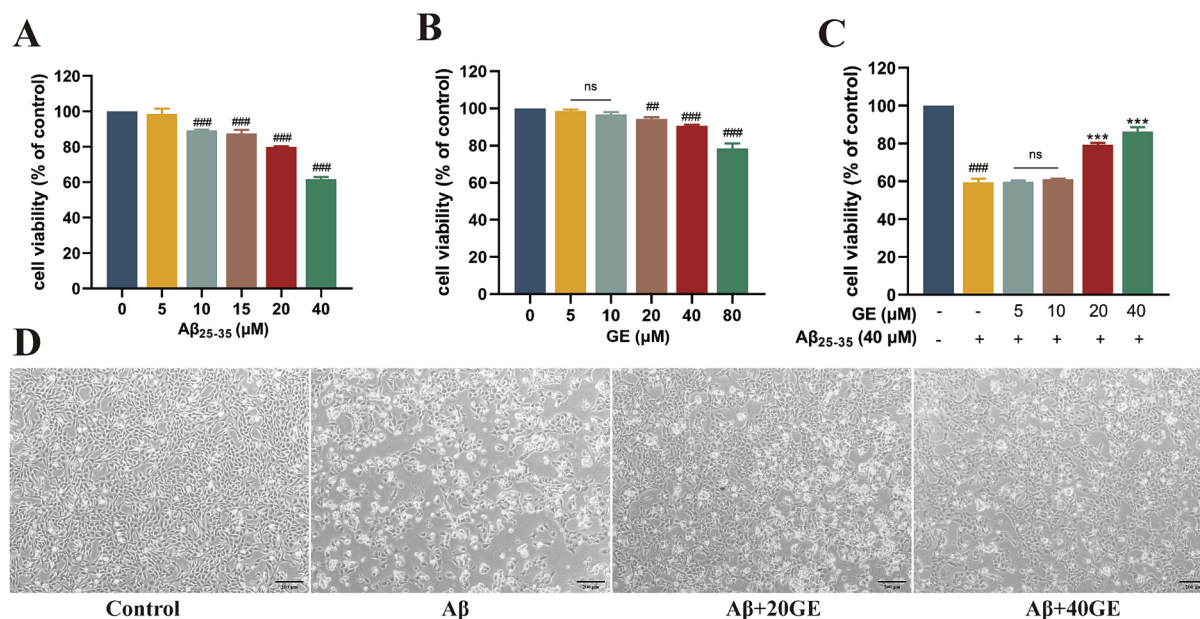


Fig. 2. GE attenuates Aβ₂₅₋₃₅-induced HT22 cell viability. (A) The effect of Aβ₂₅₋₃₅ on cell viability was examined in HT22 cells by treating them with indicated concentrations for 24 h, followed by a CCK-8 assay. (B) Cell viability in HT22 cells was evaluated using a CCK-8 assay after 24 h incubation with different concentrations of GE. (C) HT22 cells were pretreated with GE for 1 h and then incubated with Aβ₂₅₋₃₅ for 24 h. Cell viability was determined by a CCK-8 assay. (D) Observation of cell morphology with phase-contrast microscopy (scale bar: 200 μm). Data are presented as mean ± SEM. One-way analysis of variance. $n = 3$, ### $P < 0.001$ vs. control group; *** $P < 0.001$ vs. Aβ₂₅₋₃₅ group.

autophagy flux) was utilized to block autophagy in HT22 cells. Our results showed that cotreatment with CQ slightly increased LC3-II (Fig. 5A) in Aβ-induced HT22 cells, indicating that Aβ₂₅₋₃₅ treatment caused a defective autophagy flux in HT22 cells. In the western blot analysis, the decreased expression of Beclin-1 and the increased expression of p62 proteins provide evidence that Aβ₂₅₋₃₅ inhibits cellular autophagy. (Fig. 5A–F). Immunofluorescence staining of LC3 protein expression in cells yielded consistent results, demonstrating a significant reduction in fluorescence intensity in cells treated with Aβ₂₅₋₃₅ (Fig. 5G). Despite this, pretreatment with GE overturned the Aβ₂₅₋₃₅-induced upregulation of p62 protein expression and restored the conversion of LC3I to LC3II, as well as the Beclin-1 protein expression. Furthermore, it also restored intracellular LC3 levels. These results display that GE reinstates cellular autophagy in HT22 cells, exerting neuroprotective consequences.

3.5. GE activates PINK1/Parkin-mediated mitophagy in HT22 cells

To begin with, we identified 61 drug targets for GE from the TCMSP database, while a comprehensive set of 1,912 CE-related targets was obtained from the DisGeNET and GeneCards databases. By visualizing the overlapping genes in a Venn diagram (Fig. 6A), we discovered a shared pool of 26 genes between GE and AD. Subsequently, these 26 genes were uploaded to the STRING website, enabling the generation of a PPI network diagram (Fig. 6B). The PPI network obtained the apoptosis-specific gene Bcl-2 and age-related genes MMP family genes. To gain additional insight into the therapeutic mechanisms of GE in treating AD, we further explored these 26 common genes using the DAVID database. The analysis yielded notable enrichment in 76 biological processes (BP), 23 cellular components (CC), and 17 molecular functions (MF). By visualizing the 15 most significantly enriched terms in each category, as determined by the smallest p -values (Fig. 6C), we could effectively portray the outcomes. The GO enrichment results shed light on the functional relevance of GE-targeted genes in AD, revealing their association with critical biological processes such as neuronal apoptosis and the response to β-amyloid. Notably, the examination of cellular components highlighted the involvement of lysosomes and the

outer mitochondrial membrane, implicating these subcellular structures in the therapeutic implications of GE on AD.

The visualization of these interactions through STRING and Cytoscape 3.7.1 facilitated the identification of the PINK1/Parkin signaling pathway (Fig. 6D). To provide further support for the therapeutic action of GE, virtual docking studies were conducted to investigate the interaction between PINK1, Parkin, and GE. A binding energy lower than -5.0 kcal/mol is generally indicative of a favorable binding affinity between ligands [29]. In the case of GE's interaction with PINK1, it exhibited a binding energy of -8.0 kcal/mol. The docking pocket involved residues TYR-102, LYS-336, ASP-334, ASN-170, and ALA-171 (Fig. 6E). Similarly, when interacting with Parkin, GE demonstrated a binding energy of -6.0 kcal/mol. The binding pocket in this case included residues ASP-184, HIS-227, GLN-252, and ARG-256 (Fig. 6F). Thus, these results signified that GE exhibits a favorable binding affinity with both PINK1 and Parkin proteins. This analysis contributes valuable supportive evidence for the mechanism of action of GE as a potential therapeutic agent.

To examine the potential protective role of GE against Aβ₂₅₋₃₅-induced cell injury via the PINK1/Parkin-mediated signaling pathway, the mitophagy inhibitor called CsA and Mdivi-1 were employed to block intracellular mitophagy. The results from western blot indicated that the expression of PINK1 and Parkin proteins diminished in the Aβ₂₅₋₃₅ group compared to the control group. Alternatively, GE dramatically elevated the PINK1 and Parkin proteins expression. Furthermore, our results indicated that the mitophagy inhibitor CsA could suppress the expression of PINK1 and Parkin proteins in GE-treated Aβ-induced HT22 cells, while Mdivi-1 showed no significant effect (Fig. 7A and B). Additionally, we extracted mitochondrial proteins from cells in each group for western blot. The results revealed that the expression of PINK1 and Parkin proteins were decreased in Aβ-induced HT22 cells, whereas pretreatment with GE enhanced the expression of PINK1 and Parkin proteins in Aβ-induced HT22 cells. Moreover, the beneficial effects of GE were blocked by CsA, while no significant difference was observed with Mdivi-1 (Fig. 7C and D). Subsequently, immunofluorescence was employed to examine the co-localization of mitochondria (labeled with red fluorescence) and Parkin (labeled with green fluorescence). In the Aβ₂₅₋₃₅

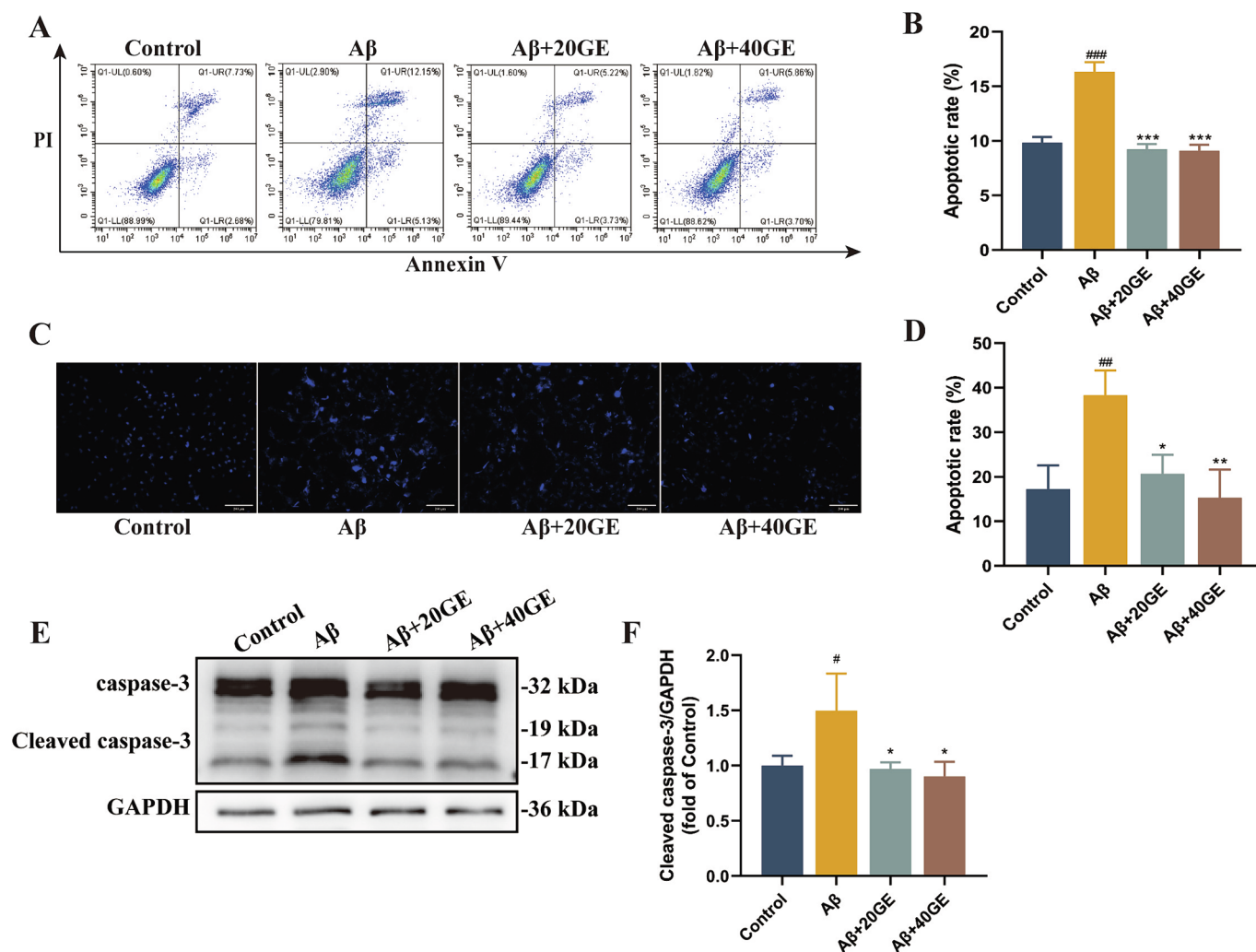


Fig. 3. GE alleviates A β_{25-35} -induced apoptosis. The Control group received no treatment, while the A β group was incubated solely with a concentration of 40 μ M A β_{25-35} for 24 h. After pre-treating HT22 cells with concentrations of 20 or 40 μ M GE for 1 h, the cells were co-incubated with A β_{25-35} (40 μ M) for 24 h. (A) HT22 cells were labeled with Annexin V-FITC/PI and detected by flow cytometry. (B) Apoptosis rate was calculated using Annexin V-FITC/PI. (C) HT22 cells were stained with Hoechst 33,342 and detected by fluorescence microscopy (scale bar: 100 μ m). (D) Apoptosis rate was calculated using Hoechst 33342. (E) Bands of Cleaved caspase-3 proteins. GAPDH was used as the loading control. (F) Protein expression levels of Cleaved caspase-3. Data are presented as mean \pm SEM. One-way analysis of variance. $n = 3$, # $P < 0.05$, ## $P < 0.01$, ### $P < 0.001$ vs. control group; * $P < 0.05$, ** $P < 0.01$, *** $P < 0.001$ vs. A β_{25-35} group.

group, the co-localization of mitochondria and Parkin was significantly reduced. Conversely, following treatment with GE, the co-localization of mitochondria and Parkin substantially increased, indicating an overall activation of mitophagy (Fig. 7E–G). The addition of CsA led to a decrease in the co-localization of mitochondria and Parkin, suggesting that CsA eliminated the protective property of GE against A β_{25-35} -induced damage. These findings provided further evidence supporting the involvement of the PINK1/Parkin-mediated signaling pathway and the activation of mitophagy in the protective action of GE against A β_{25-35} -induced cell injury.

Furthermore, we investigated the impact of adding CsA and Mdivi-1 to HT22 cells on cell morphology, apoptosis, oxidative stress, and mitochondrial function. The inclusion of CsA resulted in a reduction in neuronal density, an escalation in the rate of cell apoptosis, heightened levels of ROS, and impaired mitochondrial function, as compared to the group of A β -induced HT22 cells treated with GE (Fig. 8). However, there was no significant difference with the addition of Mdivi-1. These findings strongly signified that the activation of PINK1/Parkin-mediated mitophagy by GE effectively reinstates the damage inflicted by A β_{25-35} .

4. Discussion

Although the detailed mechanisms underlying the pathogenesis of AD remain unclear, there is substantial evidence suggesting that impaired mitochondria may play a critical role [30]. Damaged mitochondria are typically degraded through mitophagy, with the PINK1 pathway on the outer mitochondrial membrane being the most common autophagic pathway [9]. In this study, we identified that GE restores cellular vitality and reduces apoptosis induced by A β_{25-35} by restoring MMP and alleviating oxidative stress. Moreover, GE counteracted the neurotoxic results of A β_{25-35} by activating PINK1/Parkin-mediated mitophagy. Thus, the study not only supports the involvement of mitochondrial impairment in the pathogenesis of AD but also highlights the potential therapeutic outcomes of GE in treating AD.

Numerous studies have pointed out the significant therapeutic potential of natural extracts in slowing down the progression of AD [31,32]. GE, derived from the fruit of *Gardenia jasminoides*, has been reported to improve cognitive abilities in AD models by suppressing oxidative stress and neuroinflammation [33,34]. In this research, our primary focus was on investigating the antioxidative stress and autophagy effects of GE, particularly in relation to mitophagy. We utilized

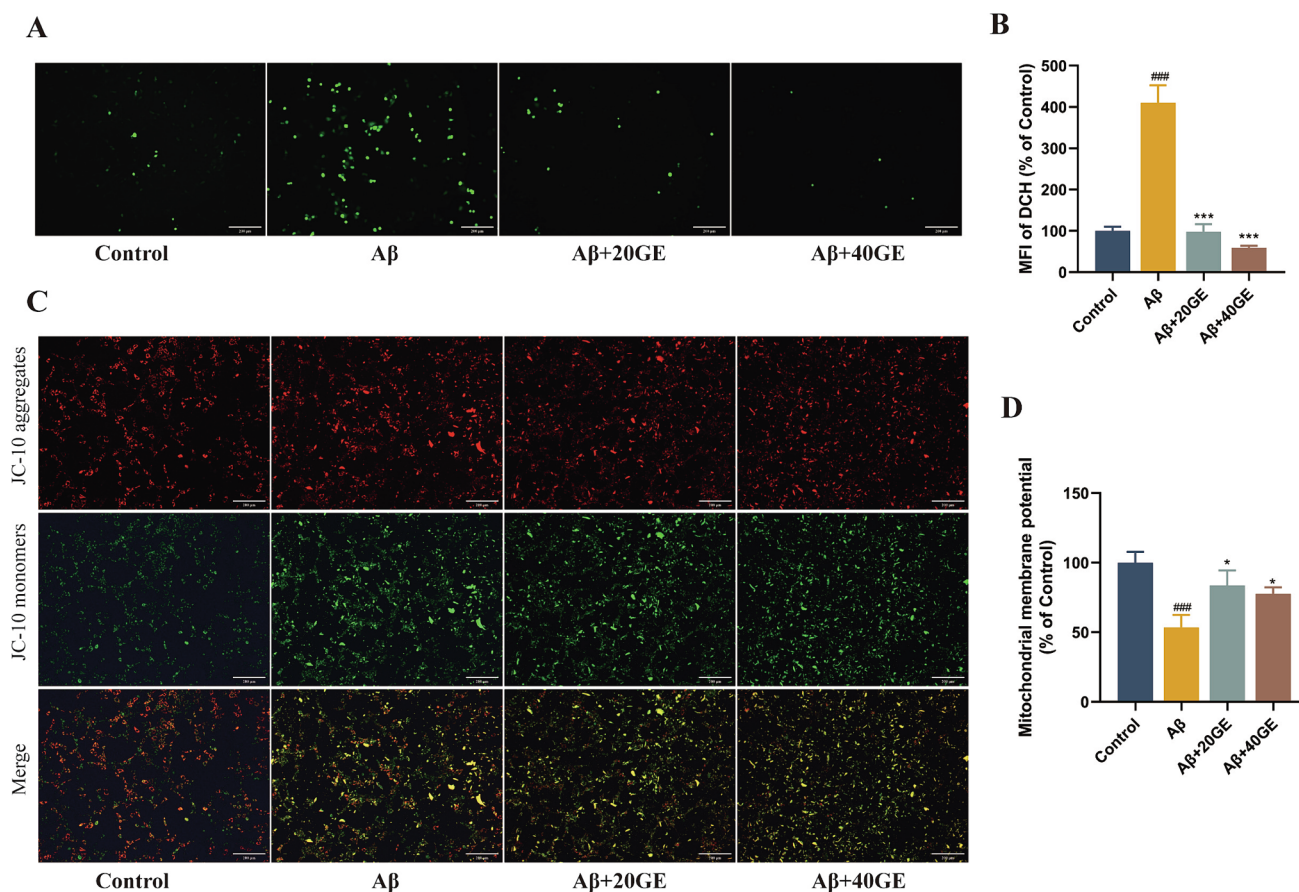


Fig. 4. GE mitigates A β_{25-35} -induced impairment of mitochondrial function and oxidative stress levels. The Control group received no treatment, while the A β group was incubated solely with a concentration of 40 μ M A β_{25-35} for 24 h. After pre-treating HT22 cells with concentrations of 20 or 40 μ M GE for 1 h, the cells were co-incubated with A β_{25-35} (40 μ M) for 24 h. (A) ROS image generated by DCFH-DA staining (scale bar: 200 μ m). (B) Quantitative analysis of mean fluorescence density of ROS. (C) The resulting MMP images were stained with JC-10 (scale bar: 200 μ m). (D) Quantitative analysis of red/green fluorescence intensity ratio. Data are presented as mean \pm SEM. One-way ANOVA analysis of variance. $n = 3$, ^{###} $P < 0.001$ vs. control group; ^{*} $P < 0.05$, ^{***} $P < 0.001$ vs. A β_{25-35} group. (For interpretation of the references to colour in this figure legend, the reader is referred to the web version of this article.)

A β_{25-35} to induce neurotoxicity, establishing a *in vitro* AD model. Through the assessment of cell viability and apoptosis, we validated that A β_{25-35} indeed reduced cell viability and increased apoptosis, consistent with our previous findings [20,35]. Treatment with GE enhanced cell viability in the presence of A β_{25-35} and restored neuronal density. Furthermore, flow cytometry and western blot provided additional evidence for the beneficial repercussions of GE in mitigating cell apoptosis.

Mitochondrial dysfunction leads to a cascade of cellular events, such as decreased ATP production and increased ROS generation [36]. Neurons are particularly vulnerable to damage caused by mitochondrial dysfunction with their high energy demands [37]. Impaired mitochondria can disrupt the expression of crucial proteins in the electron transport chain, elevate oxidative stress, and ultimately trigger cell apoptosis [38,39]. Impaired energy metabolism is a notable characteristic preceding the clinical onset of neurodegenerative disorders [40], and both mitochondrial bioenergetics and oxidative stress abnormalities can contribute to and exacerbate neuronal dysfunction and neurodegeneration [10]. As a natural antioxidant [34], GE exhibits considerable potential in counteracting oxidative stress and mitochondrial dysfunction in various neurodegenerative conditions [41–43]. Studies have revealed that GE can shield neurons from the oxidative stress and disruption of axonal mitochondrial transport induced by A β , thereby enhancing synaptic function [44]. By assessing ROS and MMP levels, we observed a striking elevation in oxidative stress and a notable reduction in MMP in A β_{25-35} -induced cells as compared to the control group. Pre-treatment with GE overturned the effects induced by A β_{25-35} , indicating

its capacity to restore mitochondrial dysfunction and exert antioxidative consequences.

Autophagy is a fundamental cellular process responsible for the degradation of cellular proteins or organelles through their sequestration and subsequent fusion with lysosomes, leading to their degradation [45]. Damaged mitochondria are typically eliminated through mitophagy to maintain cellular energy balance [46]. Failure to remove damaged mitochondria through degradation can result in the excessive aggregation of ROS, leading to oxidative stress-induced injury and cell apoptosis [47]. Numerous studies have indicated that disruption of autophagic flux leads to neuronal cell damage and death in the brains of patients with neurodegenerative diseases [48,49]. Cytoplasmic LC3I conjugates with phosphatidylethanolamine to form LC3II during the autophagic process, which is recruited and integrated into the autophagosome membrane [50]. The ratio of LC3II to LC3I serves as an indicator of autophagic activity. Beclin-1 has been shown to reduce cell apoptosis and enhance autophagy when overexpressed as a critical regulator of autophagy [51]. The p62 protein acts as an autophagic receptor that its level is inversely proportional to autophagic efficiency. It is usually used to estimate autophagic flux. Additionally, p62 can be phosphorylated in PRKN-dependent mitophagy, facilitating the removal of dysfunctional mitochondria [52]. Our data showed that CQ slightly increased LC3-II in A β -induced HT22 cells through blocking autophagy flux. However, GE increased the expression of LC3II and Beclin-1 in A β_{25-35} -treated HT22 cells while reducing the p62 protein expression, suggesting that GE has the potential to mitigate A β_{25-35} -induced

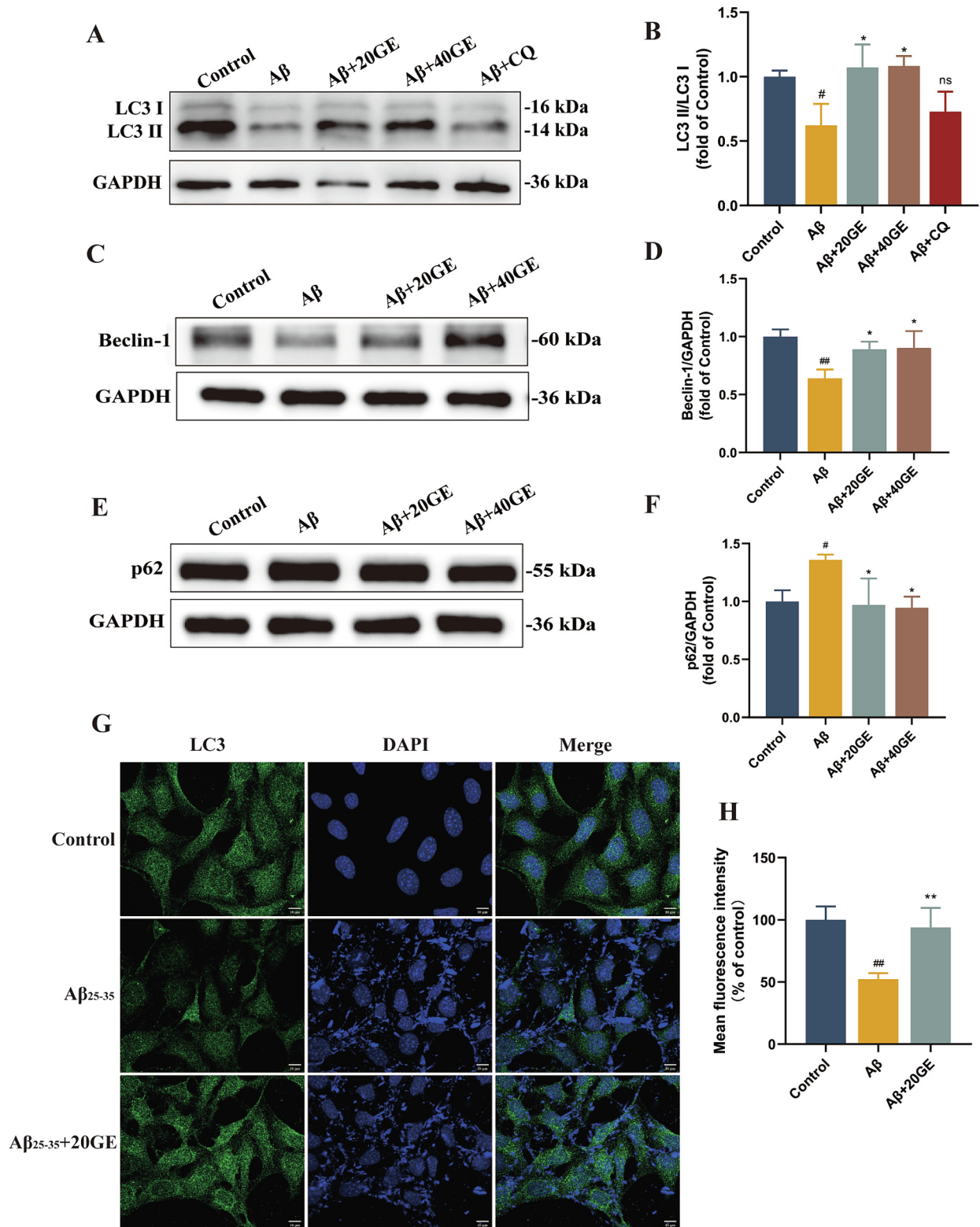


Fig. 5. GE reverses A β ₂₅₋₃₅-induced inhibition of autophagy. The Control group received no treatment, while the A β group was incubated solely with a concentration of 40 μ M A β ₂₅₋₃₅ for 24 h. After pre-treating HT22 cells with concentrations of 20 or 40 μ M GE for 1 h, the cells were co-incubated with A β ₂₅₋₃₅ (40 μ M) for 24 h. Chloroquine (30 μ M) and 40 μ M A β ₂₅₋₃₅ were incubated for 24 h. Bands of LC3 (A), Beclin-1 (C) and p62 (E) proteins. GAPDH was used as the loading control. Protein expression levels of LC3 (B), Beclin-1 (D) and p62 (F). (G) Treated cells were stained with autophagy marker LC3 (green). One representative image of three experiments is shown (scale bar: 10 μ m). (H) Mean fluorescence intensity of LC3. Data are presented as mean \pm SEM. One-way ANOVA analysis of variance. $n = 3$, # $P < 0.05$, ## $P < 0.01$ vs. control group; * $P < 0.05$, ns, ** $P < 0.01$ vs. A β ₂₅₋₃₅ group. (For interpretation of the references to colour in this figure legend, the reader is referred to the web version of this article.)

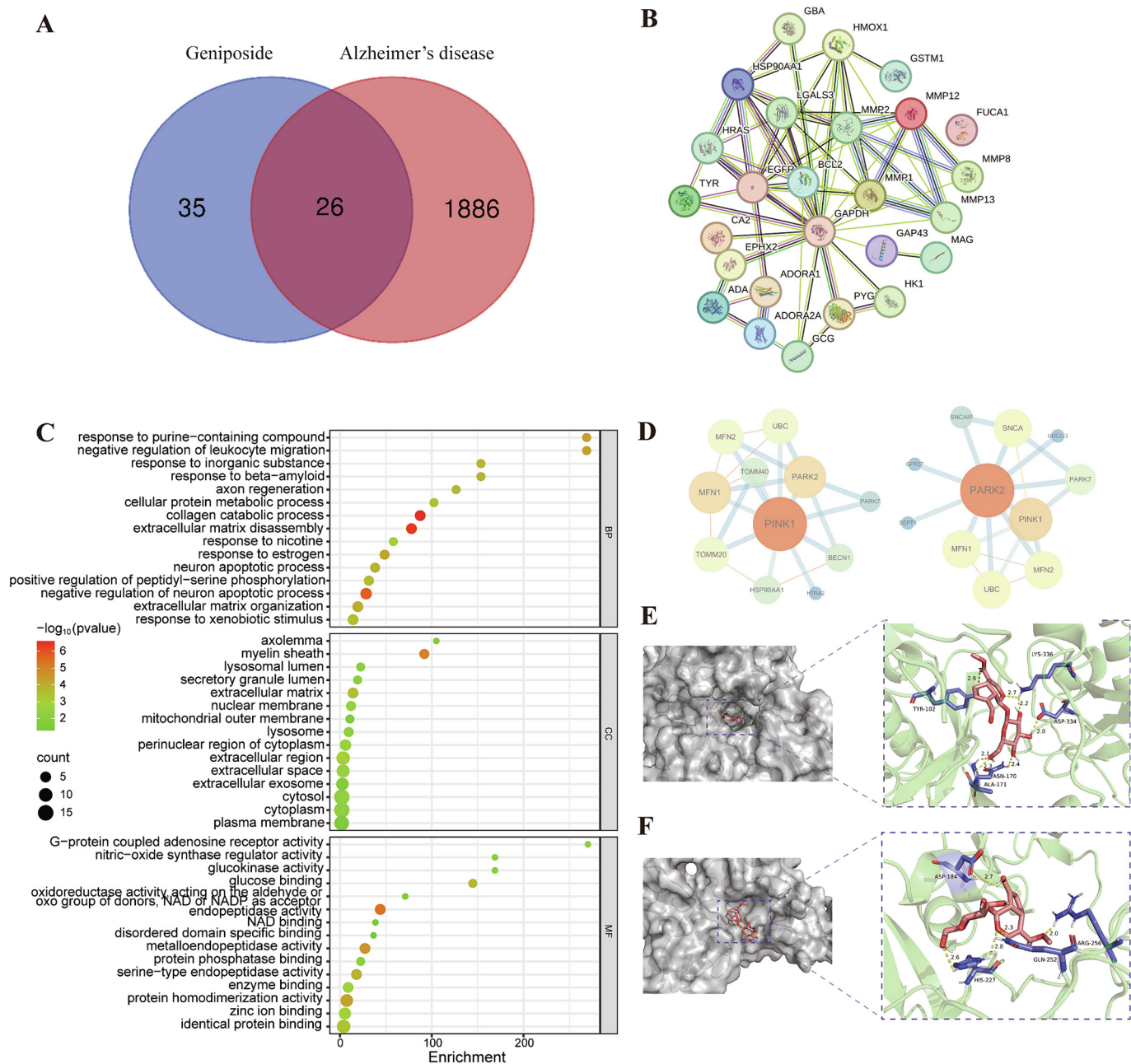


Fig. 6. Network pharmacology and molecular docking. (A) Venn diagram of gene intersection between GE and AD. (B) PPI network of intersection genes. (C) GO enrichment analysis of intersection genes. (D) PINK1 and Parkin proteins by STRING database. (E) Docking complex of PINK1 protein (6EQI) with GE with Molecular docking. (F) Docking complex of Parkin protein (4I1H) with GE with Molecular docking.

autophagic impairment.

PINK1 is a protein located on the outer membrane of mitochondria. In healthy mitochondria, PINK1 is transported to the inner membrane where it undergoes cleavage and subsequent degradation. Nevertheless, in the case of mitochondrial damage and a decrease in MMP, PINK1 is unable to enter the inner membrane and instead accumulates on the outer membrane. This accumulation triggers the activation and recruitment of Parkin protein, which in turn promotes mitophagy. The process involves the fusion of mature autophagosomes with lysosomes, forming autolysosomes where degradation takes place [8]. Mitophagy impairment has been observed in the hippocampus of AD patients, human AD neurons derived from induced pluripotent stem cells, and animal models of AD to varying extents [10]. The results of GO enrichment analysis included responses to β -amyloid and lysosomes and mitochondrial outer membrane, confirming the relationship between GE

and AD mitophagy. The interaction analysis between PINK1, Parkin, and GE had revealed a strong association. To further investigate the effects of GE on mitophagy, protein expression was analyzed through western blot, and autophagosomes and mitochondria were labeled and observed using confocal microscopy. The results demonstrated that GE could enhance mitophagy in HT22 cells treated with $A\beta_{25-35}$. As mitophagy inhibitors, CsA and Mdivi-1 have distinct mechanisms of action and target proteins. CsA inhibits mitophagy by targeting the mitochondrial permeability transition pore, while Mdivi-1 indirectly affects mitophagy by targeting mitochondrial division and fission processes [53,54]. Our results revealed that the administration of the mitophagy inhibitor CsA prevented the increased expression of PINK1 and Parkin induced by GE, indicating the critical role of GE in mitophagy. CsA also overturned the influences of GE on reducing apoptosis rates and oxidative stress, as well as increasing MMP. However, the inhibitory effects of Mdivi-1 do not

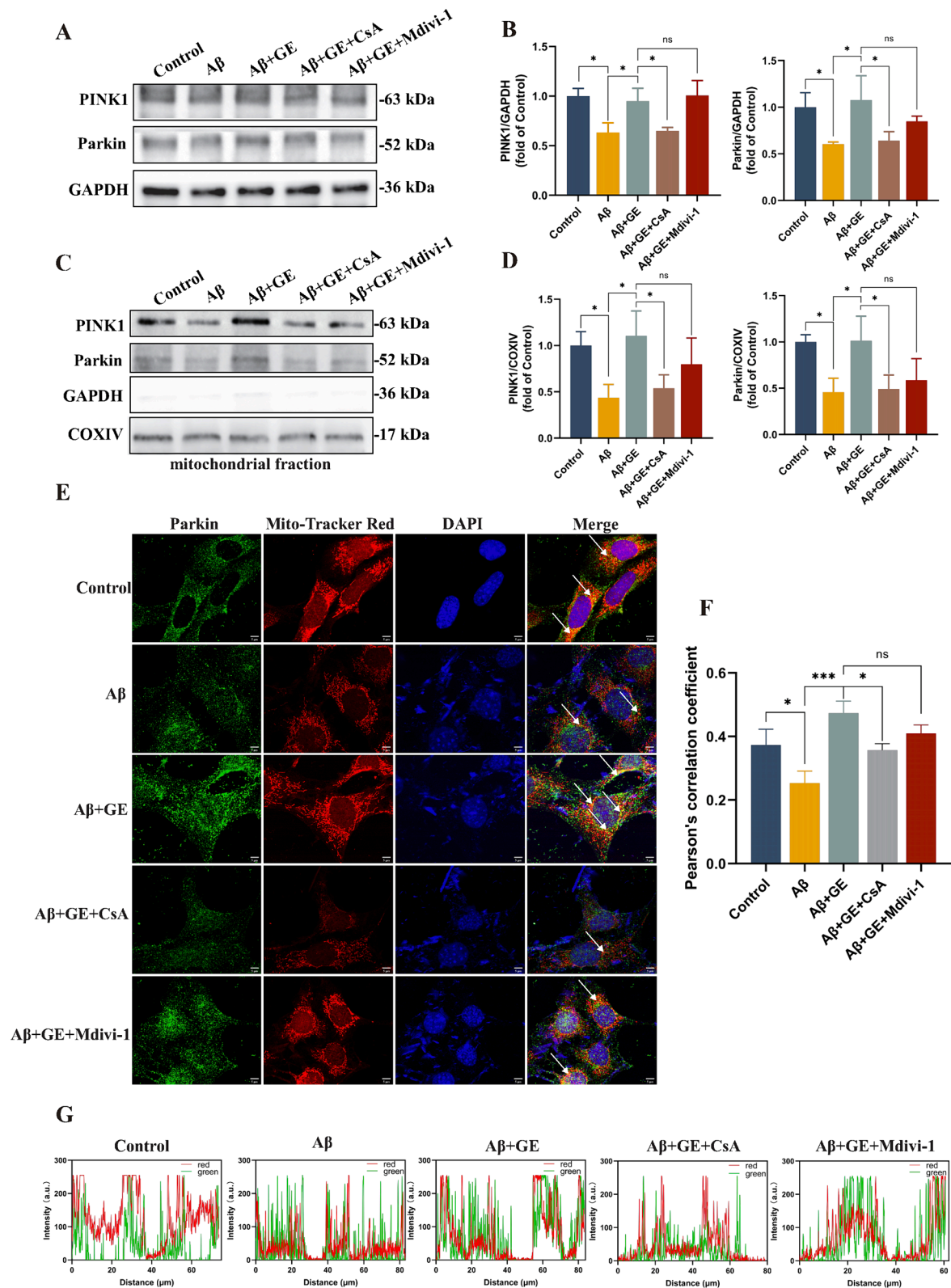


Fig. 7. Effect of GE on the mitophagy of HT22 cells induced by A β_{25-35} . The Control group received no treatment, while the A β group was incubated solely with a concentration of 40 μ M A β_{25-35} for 24 h. After pre-treating HT22 cells with concentrations of 20 μ M GE for 1 h, the cells were co-incubated with A β_{25-35} (40 μ M) for 24 h. After pre-treating HT22 cells with a concentration of 20 μ M GE for 1 h, the cells were co-incubated with 40 μ M A β_{25-35} for 24 h in the presence of the mitophagy inhibitors Csa (5 μ M) or Mdivi-1 (5 μ M). (A) The PINK1 and Parkin expression were analyzed by Western blot. (B) Protein expression levels of PINK1 and Parkin. (C) The PINK1 and Parkin expression in the mitochondrial fraction were analyzed by Western blot. (D) Protein expression levels of PINK1 and Parkin in the mitochondrial fraction. (E) Treated cells were stained with mitophagy marker Parkin (green) and mitochondria marker Mito (red). One representative image of three experiments is shown (scale bar: 5 μ m). (F) Intensity of red and green fluorescence. (G) Quantitative analysis of Pearson's correlation coefficient. Data are presented as mean \pm SEM. One-way ANOVA analysis of variance. $n = 3$, ns means no significant difference; * $P < 0.05$, *** $P < 0.001$. (For interpretation of the references to colour in this figure legend, the reader is referred to the web version of this article.)

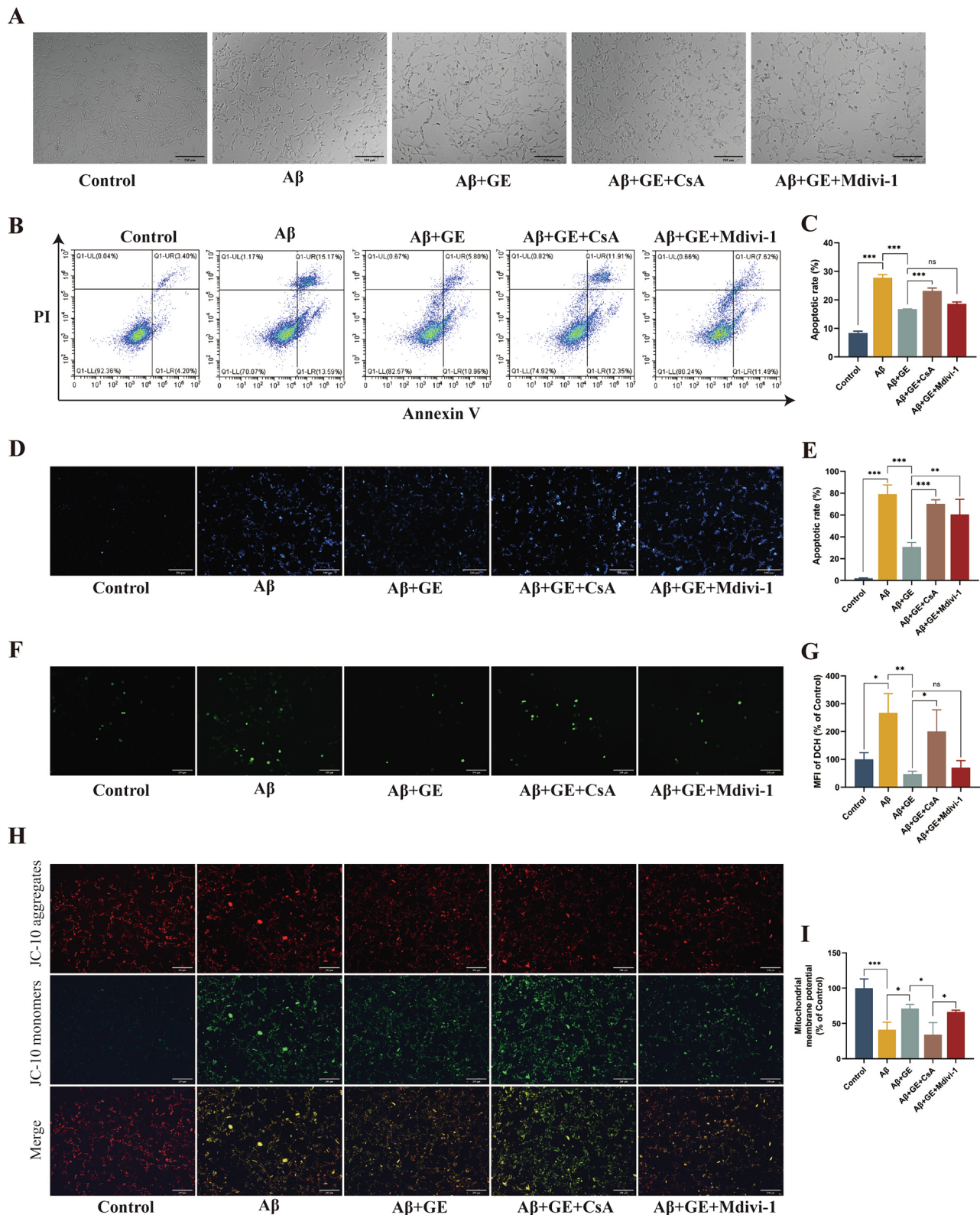


Fig. 8. Effect of GE on Aβ₂₅₋₃₅-induced cell morphology, apoptosis, oxidative stress, and mitochondrial function by adding CsA or Mdivi-1. The Control group received no treatment, while the Aβ group was incubated solely with a concentration of 40 μM Aβ₂₅₋₃₅ for 24 h. After pre-treating HT22 cells with concentrations of 20 μM GE for 1 h, the cells were co-incubated with Aβ₂₅₋₃₅ (40 μM) for 24 h. After pre-treating HT22 cells with a concentration of 20 μM GE for 1 h, the cells were co-incubated with 40 μM Aβ₂₅₋₃₅ for 24 h in the presence of the mitophagy inhibitors CsA (5 μM) or Mdivi-1 (5 μM). (A) Observation of cell morphology with phase-contrast microscopy (scale bar: 200 μm). (B) Detection of apoptosis rate by flow cytometry and Hoechst 33,342 staining to assess apoptotic morphology (scale bar: 200 μm). (C) Quantitative analysis of apoptosis rate. (D) ROS image generated by DCFH-DA staining (scale bar: 200 μm). (E) Quantitative analysis of mean fluorescence density of ROS. (F) The resulting MMP images were stained with JC-10 (scale bar: 200 μm). (G) Quantitative analysis of the red/green fluorescence intensity ratio. Data are presented as mean ± SEM. One-way ANOVA analysis of variance. *n* = 3, ns means no significant difference; **P* < 0.05, ***P* < 0.01, ****P* < 0.001. (For interpretation of the references to colour in this figure legend, the reader is referred to the web version of this article.)

exhibit significant differences. The above results indicated that GE could activate mitophagy in A β -induced HT22 cells. The main mechanism may be to regulate the modulation of mitochondrial permeability transition pore, affecting the level of autophagy and mediating the protective effects of the PINK1/Parkin pathway on HT22 cells.

Based on the above, we have elucidated the anti-dementia consequences of GE in HT22 cells. Our research provides compelling experimental evidence supporting the potential use of these natural bioactive compounds and their corresponding medicinal and edible plants in the fight against dementia. Nonetheless, it is essential to recognize and address specific limitations in the research findings. Firstly, our research primarily relied on an in vitro system, and further investigations using animal models are necessary to validate the therapeutic efficacy of GE for preventing impacts on neurodegeneration. Secondly, the issue of GE's bioavailability in vivo warrants consideration to fully understand its potential as a treatment option.

In summary, our study presented compelling evidence supporting the defense mechanism against the neurotoxicity of GE against A β ₂₅₋₃₅-induced HT22 cell damage. The mechanism underlying this protective action appears to involve the activation of mitophagy, leading to the restoration of MMP, alleviation of oxidative stress, and attenuation of cell apoptosis. These discoveries reveal new understandings of the neurotoxicity of A β ₂₅₋₃₅ and highlight the potential of GE as a protective agent in HT22 cells.

Funding

This work was supported by the Natural Science Foundation of Guangdong Provincial, China (2019A1515011414 and 2023A1515011136) and the Administration of Traditional Chinese Medicine of Guangdong Province, China (20211072).

CRediT authorship contribution statement

Jiayi Ye: Writing – review & editing, Writing – original draft, Project administration, Funding acquisition, Conceptualization. **Jiaying Wu:** Visualization, Methodology, Formal analysis. **Liang Ai:** Resources, Methodology. **Min Zhu:** Resources, Methodology. **Yun Li:** Visualization, Resources. **Dong Yin:** Resources, Project administration. **Qihui Huang:** Writing – review & editing, Project administration, Funding acquisition, Conceptualization.

Declaration of competing interest

The authors declare that they have no known competing financial interests or personal relationships that could have appeared to influence the work reported in this paper.

Data availability

No data was used for the research described in the article.

References

- [1] J. Cummings, New approaches to symptomatic treatments for Alzheimer's disease, *Mol. Neurodegener.* 16 (2021) 2, <https://doi.org/10.1186/s13024-021-00424-9>.
- [2] M. Zhou, H. Wang, X. Zeng, P. Yin, J. Zhu, W. Chen, X. Li, et al., Mortality, morbidity, and risk factors in China and its provinces, 1990–2017: a systematic analysis for the global burden of disease study 2017, *Lancet.* 394 (2019) 1145–1158, [https://doi.org/10.1016/S0140-6736\(19\)30427-1](https://doi.org/10.1016/S0140-6736(19)30427-1).
- [3] Y.Q. Zhang, C.F. Wang, G. Xu, Q.H. Zhao, X.Y. Xie, H.L. Cui, Y. Wang, et al., Mortality of Alzheimer's disease patients: a 10-year follow-up pilot study in Shanghai, *Can. J. Neurol. Sci.* 47 (2020) 226–230, <https://doi.org/10.1017/cjn.2019.333>.
- [4] R. Briggs, S.P. Kenedy, D. O'Neill, Drug treatments in Alzheimer's disease, *Clin. Med. (lond)* 16 (2016) 247–253, <https://doi.org/10.7861/clinmedicine.16-3-247>.
- [5] J.S. Kerr, B.A. Adriaanse, N.H. Greig, M.P. Mattson, M.Z. Cader, V.A. Bohr, E. F. Fang, Mitophagy and alzheimer's disease: cellular and molecular mechanisms, *Trends. Neurosci.* 40 (2017) 151–166, <https://doi.org/10.1016/j.tins.2017.01.002>.
- [6] J. Yin, E.M. Reiman, T.G. Beach, G.E. Serrano, M.N. Sabbagh, M. Nielsen, R. J. Caselli, et al., Effect of ApoE isoforms on mitochondria in Alzheimer disease, *Neurology.* 94 (2020) e2404–e2411, <https://doi.org/10.1212/WNL.00000000000009582>.
- [7] J.M. Perez Ortiz, R.H. Swerdlow, Mitochondrial dysfunction in Alzheimer's disease: role in pathogenesis and novel therapeutic opportunities, *Br. J. Pharmacol.* 176 (2019) 3489–3507, <https://doi.org/10.1111/bph.14585>.
- [8] L.E. Fritsch, M.E. Moore, S.A. Sarraf, A.M. Pickrell, Ubiquitin and receptor-dependent mitophagy pathways and their implication in neurodegeneration, *J. Mol. Biol.* 432 (2020) 2510–2524, <https://doi.org/10.1016/j.jmb.2019.10.015>.
- [9] J.A. Pradeepkiran, P.H. Reddy, Defective mitophagy in Alzheimer's disease, *Ageing. Res. Rev.* 64 (2020) 101191, <https://doi.org/10.1016/j.arr.2020.101191>.
- [10] E.F. Fang, Y. Hou, K. Palikaras, B.A. Adriaanse, J.S. Kerr, B. Yang, S. Lautrup, et al., Mitophagy inhibits amyloid- β and tau pathology and reverses cognitive deficits in models of Alzheimer's disease, *Nat. Neurosci.* 22 (2019) 401–412, <https://doi.org/10.1038/s41593-018-0332-9>.
- [11] R. Ai, X.X. Zhuang, A. Anisimov, J.H. Lu, E.F. Fang, A synergized machine learning plus cross-species wet-lab validation approach identifies neuronal mitophagy inducers inhibiting Alzheimer disease, *Autophagy.* 18 (2022) 939–941, <https://doi.org/10.1080/15548627.2022.2031382>.
- [12] E.J. Seo, N. Fischer, T. Efferth, Phytochemicals as inhibitors of NF- κ B for treatment of Alzheimer's disease, *Pharmacol. Res.* 129 (2018) 262–273, <https://doi.org/10.1016/j.phrs.2017.11.030>.
- [13] G. Zhang, J.L. He, X.Y. Xie, C. Yu, LPS-induced iNOS expression in N9 microglial cells is suppressed by geniposide via ERK, p38 and nuclear factor- κ B signaling pathways, *Int. J. Mol. Med.* 30 (2012) 561–568, <https://doi.org/10.3892/ijmm.2012.1030>.
- [14] L.X. Guo, J.H. Liu, Z.N. Xia, Geniposide inhibits CoCl₂-induced PC12 cells death via the mitochondrial pathway, *Chin. Med. J. (engl)* 122 (2009) 2886–2892.
- [15] P. Sun, H. Ding, M. Liang, X. Li, W. Mo, X. Wang, Y. Liu, et al., Neuroprotective effects of geniposide in SH-SY5Y cells and primary hippocampal neurons exposed to A β ₄₂, *Biomed. Res. Int.* 2014 (2014) 284314, <https://doi.org/10.1155/2014/284314>.
- [16] C. Lv, X. Liu, H. Liu, T. Chen, W. Zhang, Geniposide attenuates mitochondrial dysfunction and memory deficits in APP/PS1 transgenic mice, *Curr. Alzheimer. Res.* 11 (2014) 580–587, <https://doi.org/10.2174/1567205011666140618095925>.
- [17] C. Zhao, C. Lv, H. Li, S. Du, X. Liu, Z. Li, W. Xin, et al., Geniposide protects primary cortical neurons against oligomeric A β ₁₋₄₂-induced neurotoxicity through a mitochondrial pathway, *PLoS. One.* 11 (2016) e0152551.
- [18] Z. Zhang, W. Gao, X. Wang, D. Zhang, Y. Liu, L. Li, Geniposide effectively reverses cognitive impairment and inhibits pathological cerebral damage by regulating the mTOR signaling pathway in APP/PS1 mice, *Neurosci. Lett.* 720 (2020) 134749, <https://doi.org/10.1016/j.neulet.2020.134749>.
- [19] Z. Zhang, X. Wang, D. Zhang, Y. Liu, L. Li, Geniposide-mediated protection against amyloid deposition and behavioral impairment correlates with downregulation of mTOR signaling and enhanced autophagy in a mouse model of Alzheimer's disease, *Aging. (alban NY)* 11 (2019) 536–548, <https://doi.org/10.18632/aging.101759>.
- [20] R.L. Zhang, B.X. Lei, G.Y. Wu, Y.Y. Wang, Q.H. Huang, Protective effects of berberine against β -amyloid-induced neurotoxicity in HT22 cells via the Nrf2/HO-1 pathway, *Bioorg. Chem.* 133 (2023) 106210, <https://doi.org/10.1016/j.bioorg.2022.106210>.
- [21] J. Ru, P. Li, J. Wang, W. Zhou, B. Li, C. Huang, et al., TCMSP: a database of systems pharmacology for drug discovery from herbal medicines, *J. Cheminform.* 6 (2014) 13, <https://doi.org/10.1186/1758-2946-6-13>.
- [22] E. Coudert, S. Gehant, E. de Castro, M. Pozzato, D. Baratin, T. Neto, et al., Annotation of biologically relevant ligands in UniProtKB using ChEBI, *Bioinformatics.* 39 (2023) btac793, <https://doi.org/10.1093/bioinformatics/btac793>.
- [23] J. Piñero, N. Queralt-Rosinach, À. Bravo, J. Deu-Pons, A. Bauer-Mehren, M. Baron, et al., DisGenET: a discovery platform for the dynamical exploration of human diseases and their genes, *Database (oxford)* (2015) bav028, <https://doi.org/10.1093/database/bav028>.
- [24] G. Stelzer, N. Rosen, I. Plaschkes, S. Zimmerman, M. Twik, S. Fishilevich, T. I. Stein, et al., The GeneCards Suite: From Gene Data Mining to Disease Genome Sequence Analyses, *Curr. Protoc. Bioinformatics.* 54 (2016), 1.30.1–1.30.33. doi: 10.1002/cpbi.5.
- [25] D. Szklarczyk, J. H. Morris, H. Cook, M. Kuhn, S. Wyder, M. Simonovic, A. Santos, et al., The STRING database in 2017: quality-controlled protein-protein association networks, made broadly accessible, *Nucleic. Acids. Res.* 45(2007), D362–D368. doi: 10.1093/nar/gkw937.
- [26] B. T. Sherman, M. Hao, J. Qiu, X. Jiao, M. W. Baseler, H. C. Lane, T. Imamichi, et al., DAVID: a web server for functional enrichment analysis and functional annotation of gene lists (2021 update), *Nucleic. Acids. Res.* 50(2022), W216–W221. doi: 10.1093/nar/gkac194.
- [27] S.K. Burley, C. Bhikadiya, C. Bi, S. Bittrich, L. Chen, G.V. Crichlow, C.H. Christie, et al., RCSB Protein Data Bank: powerful new tools for exploring 3D structures of biological macromolecules for basic and applied research and education in fundamental biology, biomedicine, biotechnology, bioengineering and energy sciences, *Nucleic. Acids. Res.* 49 (2021) D437–D451, <https://doi.org/10.1093/nar/gkaa1038>.
- [28] S. Kim, J. Chen, T. Cheng, A. Gindulyte, J. He, S. He, Q. Li, PubChem update: improved access to chemical data, *Nucleic. Acids. Res.* 47 (2019) D1102–D1109, <https://doi.org/10.1093/nar/gky1033>.

- [29] X. Li, S. Wei, S. Niu, X. Ma, H. Li, M. Jing, Y. Zhao, Network pharmacology prediction and molecular docking-based strategy to explore the potential mechanism of Huanglian Jiedu Decoction against sepsis, *Comput. Biol. Med.* 144 (2022) 105389, <https://doi.org/10.1016/j.combiomed.2022.105389>.
- [30] I.G. Onyango, Modulation of mitochondrial bioenergetics as a therapeutic strategy in Alzheimer's disease, *Neural. Regen. Res.* 13 (2018) 19–25, <https://doi.org/10.4103/1673-5374.224362>.
- [31] B. Dinda, M. Dinda, G. Kulsi, A. Chakraborty, S. Dinda, Therapeutic potentials of plant iridoids in Alzheimer's and Parkinson's diseases: A review, *Eur. J. Med. Chem.* 169 (2019) 185–199, <https://doi.org/10.1016/j.ejmech.2019.03.009>.
- [32] A. Dey, R. Bhattacharya, A. Mukherjee, D. Pandey, Natural products against Alzheimer's disease: Pharmaco-therapeutics and biotechnological interventions, *Biotechnol. Adv.* 35 (2017) 178–216, <https://doi.org/10.1016/j.biotechadv.2016.12.005>.
- [33] J. Liu, F. Yin, X. Zheng, J. Jing, Y. Hu, Geniposide, a novel agonist for GLP-1 receptor, prevents PC12 cells from oxidative damage via MAP kinase pathway, *Neurochem. Int.* 51 (2007) 361–369, <https://doi.org/10.1016/j.neuint.2007.04.021>.
- [34] C. Lv, L. Wang, X. Liu, S. Yan, S.S. Yan, Y. Wang, W. Zhang, Multi-faced neuroprotective effects of geniposide depending on the RAGE-mediated signaling in an Alzheimer mouse model, *Neuropharmacology.* 89 (2015) 175–184, <https://doi.org/10.1016/j.neuropharm.2014.09.019>.
- [35] X.F. Huang, J.J. Li, Y.G. Tao, X.Q. Wang, R.L. Zhang, J.L. Zhang, Z.Q. Su, et al., Geniposide attenuates A β 25–35-induced neurotoxicity via the TLR4/NF- κ B pathway in HT22 cells, *RSC. Adv.* 8 (2018) 18926–18937, <https://doi.org/10.1039/c8ra01038b>.
- [36] J. Nunnari, A. Suomalainen, Mitochondria: in sickness and in health, *Cell.* 148 (2012) 1145–1159, <https://doi.org/10.1016/j.cell.2012.02.035>.
- [37] T. Song, X. Song, C. Zhu, R. Patrick, M. Skurla, I. Santangelo, M. Green, et al., Mitochondrial dysfunction, oxidative stress, neuroinflammation, and metabolic alterations in the progression of Alzheimer's disease: A meta-analysis of in vivo magnetic resonance spectroscopy studies, *Ageing. Res. Rev.* 72 (2021) 101503, <https://doi.org/10.1016/j.arr.2021.101503>.
- [38] M.U. Rehman, N. Sehar, N.J. Dar, A. Khan, A. Arafah, S. Rashid, S.M. Rashid, et al., Mitochondrial dysfunctions, oxidative stress and neuroinflammation as therapeutic targets for neurodegenerative diseases: An update on current advances and impediments, *Neurosci. Biobehav. Rev.* 144 (2023) 104961, <https://doi.org/10.1016/j.neubiorev.2022.104961>.
- [39] H. Ullah, A. Di Minno, C. Santarcangelo, H. Khan, M. Daglia, Improvement of Oxidative Stress and Mitochondrial Dysfunction by β -Caryophyllene: A Focus on the Nervous System, *Antioxidants (basel).* 10 (2021) 546, <https://doi.org/10.3390/antiox10040546>.
- [40] W. Wang, F. Zhao, X. Ma, G. Perry, X. Zhu, Mitochondria dysfunction in the pathogenesis of Alzheimer's disease: recent advances, *Mol. Neurodegener.* 15 (2020) 30, <https://doi.org/10.1186/s13024-020-00376-6>.
- [41] C. Li, X. Wang, F. Cheng, X. Du, J. Yan, C. Zhai, J. Mu, et al., Geniposide protects against hypoxia/reperfusion-induced blood-brain barrier impairment by increasing tight junction protein expression and decreasing inflammation, oxidative stress, and apoptosis in an in vitro system, *Eur. J. Pharmacol.* 854 (2019) 224–231, <https://doi.org/10.1016/j.ejphar.2019.04.021>.
- [42] Q. Zhou, B. Chen, Y. Xu, Y. Wang, Z. He, X. Cai, Y. Qin, et al., Geniposide protects against neurotoxicity in mouse models of rotenone-induced Parkinson's disease involving the mTOR and Nrf2 pathways, *J. Ethnopharmacol.* 318 (2023) 116914, <https://doi.org/10.1016/j.jep.2023.116914>.
- [43] W. Zhang, F. Zhang, Q. Hu, X. Xiao, L. Ou, Y. Chen, S. Luo, et al., The emerging possibility of the use of geniposide in the treatment of cerebral diseases: a review, *Chin. Med.* 16 (2021) 86, <https://doi.org/10.1186/s13020-021-00486-3>.
- [44] H. Zhang, C. Zhao, C. Lv, X. Liu, S. Du, Z. Li, Y. Wang, et al., Geniposide alleviates amyloid-induced synaptic injury by protecting axonal mitochondrial trafficking, *Front. Cell. Neurosci.* 10 (2017) 309, <https://doi.org/10.3389/fncel.2016.00309>.
- [45] W. Zhang, C. Xu, J. Sun, H.M. Shen, J. Wang, C. Yang, Impairment of the autophagy-lysosomal pathway in Alzheimer's diseases: Pathogenic mechanisms and therapeutic potential, *Acta. Pharmaceutica. Sinica. b.* 12 (2022) 1019–1040, <https://doi.org/10.1016/j.apsb.2022.01.008>.
- [46] Y. Hou, X. Dan, M. Babbar, Y. Wei, S.G. Hasselbalch, D.L. Croteau, V.A. Bohr, Ageing as a risk factor for neurodegenerative disease, *Nat. Rev. Neurol.* 15 (2019) 565–581, <https://doi.org/10.1038/s41582-019-0244-7>.
- [47] M.L. Huang, S. Chiang, D.S. Kalinowski, D.H. Bae, S. Sahni, D.R. Richardson, The role of the antioxidant response in mitochondrial dysfunction in degenerative diseases: cross-talk between antioxidant defense, autophagy, and apoptosis, *Oxid. Med. Cell. Longev.* 2019 (2019) 6392763, <https://doi.org/10.1155/2019/6392763>.
- [48] Z.B. Wei, Y.F. Yuan, F. Jaouen, M.S. Ma, C.J. Hao, Z. Zhang, Q. Chen, et al., SLC35D3 increases autophagic activity in midbrain dopaminergic neurons by enhancing BECN1-ATG14-PIK3C3 complex formation, *Autophagy.* 12 (2016) 1168–1179, <https://doi.org/10.1080/15548627.2016.1179402>.
- [49] R.L. Vidal, S. Matus, L. Bargsted, C. Hetz, Targeting autophagy in neurodegenerative diseases, *Trends in Pharmacological Sciences.* 35 (2014) 583–591, <https://doi.org/10.1016/j.tips.2014.09.002>.
- [50] H.R. Pugsley, Quantifying autophagy: Measuring LC3 puncta and autolysosome formation in cells using multispectral imaging flow cytometry, *Methods.* 112 (2017) 147–156, <https://doi.org/10.1016/j.ymeth.2016.05.022>.
- [51] K. Zhang, S. Zhu, J. Li, T. Jiang, L. Feng, J. Pei, G. Wang, et al., Targeting autophagy using small-molecule compounds to improve potential therapy of Parkinson's disease, *Acta. Pharm. Sin. b.* 11 (2021) 3015–3034, <https://doi.org/10.1016/j.apsb.2021.02.016>.
- [52] J.P. Chua, H. De Calbiac, E. Kabashi, S.J. Barmada, Autophagy and ALS: mechanistic insights and therapeutic implications, *Autophagy.* 18 (2022) 254–282, <https://doi.org/10.1080/15548627.2021.1926656>.
- [53] N. Brustovetsky, J.M. Dubinsky, Limitations of cyclosporin A inhibition of the permeability transition in CNS mitochondria, *The Journal of Neuroscience : the Official Journal of the Society for Neuroscience.* 20 (2000) 8229–8237, <https://doi.org/10.1523/JNEUROSCI.20-22-08229.2000>.
- [54] E.A. Bordt, P. Clerc, B.A. Roelofs, A.J. Saladino, L. Tretter, V. Adam-Vizi, E. Chero, et al., The putative Drp1 inhibitor mdivi-1 is a reversible mitochondrial complex I inhibitor that modulates reactive oxygen species, *Developmental Cell.* 40 (2017) 583–594.e6, <https://doi.org/10.1016/j.devcel.2017.02.020>.